

Inversion of experimental data and thermal tomography using "Termo.Heat" and "Termidge" software

by VAVILOV V.P.*, KOURTENKOV D.G.*,
GRINZATO E.#, BISON P.G.#, MARINETTI S.# and BRESSAN C.#

* Tomsk Polytechnic University, Russia, 634028, Tomsk, 28, Savinykh, 3

ITEF-CNR, Corso Stati Uniti, 4, 35020-Padova, Italy

Abstract

Modern analysis of thermal NDT data involves solving direct and inverse heat transfer problems. This paper presents methodology in determining relationships between parameters in thermal test and identifying experimental data for defects characterization purpose.

1. Introduction

For a long time infrared (IR) thermograms, e.g. in medicine, building, energy producing etc., have been qualitatively evaluated by operators who performed "mental" inversion of thermal NDT (TNDT) results. With necessity to process multiple data and/or to perform quantitative estimates of inspection results the computer modeling and decision making software started to be increasingly used in TNDT (see proceedings of QIRT-92 seminar).

Computer modeling involves solutions to direct and inverse heat diffusion problems. Analytical and numerical algorithms and corresponding computer codes intended to solve direct problems are widely used in TNDT. Origin of theoretical approach accepted in this paper could be traced to earlier paper by VAVILOV and TAYLOR [1]. Inverse problems have acquired particular interest in TNDT for the last decade. Some analytical inversion expressions based on space- and time-domain analysis have become available [2].

This paper contains some results of cooperation between Tomsk Polytechnic University and ITEF-CNR in quantifying TNDT data by using two particular software packages (see also [3-7]).

2. "Termo.Heat" software

2.1. General description

Physical problem is illustrated with *figure 1*: disk-shaped specimen which contains disk-shaped defect is uniformly (or locally) heated on front (F) surface with square or periodic heat pulse. Heat exchange by free convection occurs on both front and rear (R) surfaces. Sixteen input parameters including running time are involved into consideration for one-piece specimen with anisotropy in r - and z -direction. Arbitrary number of anisotropic layers could be also considered. Related mathematical 2D problem in cylindrical coordinates was described elsewhere [6].

3D presentation of calculated temperature field is also shown in *figure 1*. Temperature values in characteristic points, profiles or total temperature data serve as output data. Practical interest have the following parameters: temperature signal over defect on both surfaces, dimensionless temperature contrast, optimum observation time and/or time evolution function.

"Termo.Heat" software is flexible enough to meet the most of practical NDT cases. The corresponding models are shown in *figure 2* (notice the possibility to introduce complimentary air layers in order to simulate surface defects, e.g. corrosion).

2.2. Example: detection of delaminations in fresco plaster

2.2.1. Direct problem

Air delaminations in ancient plaster could lead to destruction of invaluable imprinted frescos.

The colour plates of this article are on page XIV at the end of the book.

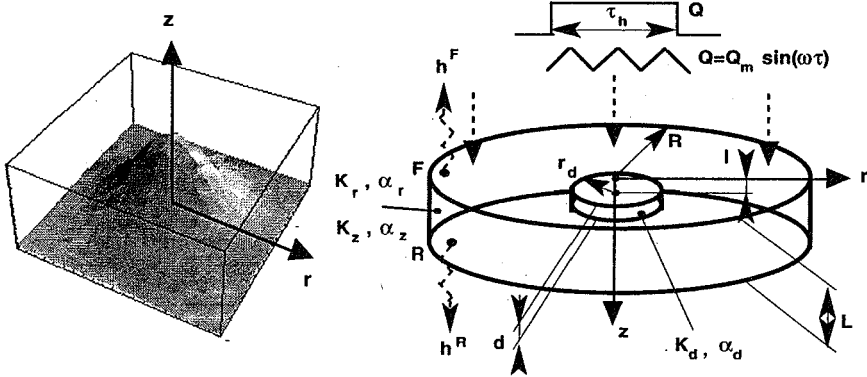


Fig.1. 2D cylindric anisotropic thermal NDT model and appearance of temperature field on front surface (arbitrary number of layers in a specimen is optional)

Nondestructive testing of such defects is possible in transient thermographic test using low-power heating. Analysis of this TNDT application has been done elsewhere [7]. Here we shall illustrate the use of "Termo.Heat" software to estimate two important inspection parameters: running temperature contrast $C_m^{(1)} = \Delta T_m(\tau_m) / T(\tau_m)$ on front surface and optimum time for its observation $\tau_m(C_m^{(1)})$.

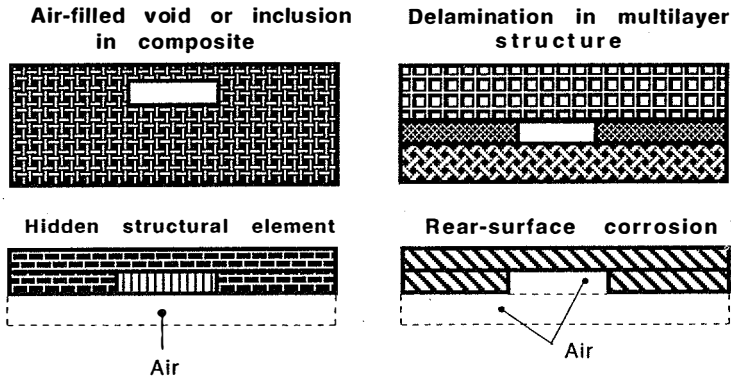


Fig.2. TNDT models related to "Termo.Heat" software

Values of temperature contrast and optimum observation time are presented in Table 1 for various values of defect radius r_d , thickness d and depth l .

2.2.2. Simple inversion of defect depth and thickness

Data in Table 1 illustrate clearly influence of defect size and depth on parameters which are recorded in experiment. Having applied to these data standard least-square fit procedure, e.g.

Table 1 Inspection parameters in the TNDT of air delaminations in plaster

(specimen thickness $L=32$ mm; specimen conductivity $K=0.48$ W/m.K and diffusivity $\alpha = 4 \times 10^{-7}$ m²s⁻¹; air delamination conductivity $K_d = 0.07$ Wm⁻¹K⁻¹ and diffusivity $\alpha_d = 25.8 \times 10^{-5}$ m²s⁻¹; heat power density 320 W m⁻²; heat pulse duration $\tau_h = 120$ s)

r_d, mm	l, mm	d, mm	$C_m^{(1)}$	τ_m, s	
38	5	1	0.305	170	
		5	0.935	230	
		10	1.232	260	
	10	1	0.182	300	
		5	0.559	380	
		10	0.729	420	
	20	1	0.063	570	
		5	0.197	670	
		10	0.271	730	
	50	5	1	0.309	180
			5	0.975	240
			10	1.292	280
10		1	0.187	310	
		5	0.610	420	
		10	0.815	470	
20		1	0.070	600	
		5	0.234	730	
		10	0.330	770	

using the "Mathematica" package, it is possible to perform analytical approximation of relevant functions. For instance, data in Table 1 could be fitted with the following functions (with accuracy not worse than 11 %):

$$C_m = 2.74e^{-0.1l} \left[1 - e^{-0.04r_d} \right] \cdot \left[1 - e^{-0.25d} \right] \tag{1}$$

$$\tau_m = 0.004 \left[1 - e^{-0.04r_d} \right] \cdot [14 + 28l] \cdot [300 + 50Ln(d)]$$

where r_d, l, d are expressed in [mm]; τ_m in [s].

Discussion on peculiarities of inverse procedures in TNDT is far beyond of the scope of this paper (we refer a reader to review paper [2]). Simple inversion formulas could be obtained if planar size of defects is neglected (e.g. in plaster this comes with defect planar size larger than 50 mm). The next assumption could be that defect depth relates mostly to heat transit time τ_m and defect thickness - to maximum signal C_m . Two simple inversion graphs $l(\tau_m)$ and $d(C_m)$ have been applied to experimental data in the inspection of a plaster specimen with unknown delamination. As the result, the size of equivalent defect has been estimated as having volume 14.9 cm³. Real defect volume after having destroyed the specimen was found to be 17 cm³ (accuracy 12 %) [7].

2.2.3. Combining maxigram and timegram

For defects with large transverse size the data in Table 1 could be represented with the set of two equations with two unknown parameters:

$$l = 0.0274 \cdot \tau_m^{0.950} \cdot C_m^{-0.226} \tag{2}$$

$$d = 0.00171 \cdot \tau_m^{1.460} \cdot C_m^{1.126}$$

where depth and thickness are expressed in [mm], time in [s]. In the range $l = 5 + 20mm$ and $d = 1 + 10mm$ (see data in Table 1) the average accuracy in determining defect depth is about 4 % (maximum error 10 %), in determining defect thickness-about 12 % (maximum 33 %). Being applied to an IR image sequence Eqs.(2) will produce images which could be called "depthgram" and "thicknessgram". In their turn distributions of C_m and τ_m are called "maxigrams" and "timegrams" and used in the "Termidge" software for tomography and defect characterization.

It is important that calibration functions (2) are individual, i.e. they are valid only for the particular specimen.

2.3. Example: detection of Teflon inserts in CFRP

2.3.1 Direct problem

The approach above has been applied to standard carbon fibre reinforced plastic (CFRP) specimen described in [8]. The specimen of thickness 5.25 mm contained square-shaped Teflon inserts at various depth. Computations have been made with "Termo.Heat" program for defects with the same equivalent transverse area and placed at the same depth as in the real specimen. Since there is a strong suspect that in specimens like this inserting Teflon inserts could also cause air delaminations the calculation has been made for both air and Teflon defects. Results are in the Table 2 (notice that running contrast in this case is replaced with normalized contrast $C_m^{(2)} = \Delta T_m / T_m$, where T_m -maximum excess temperature which occurs at the end of pulse).

2.3.2 Inversion of defect parameters

Having noticed that optimum observation time depends mostly on defect depth we have found the following inversion formulas:

$$\text{for air defects} \quad l = -0.005 + 0.177 \cdot \tau_m + 0.00424 \tau_m^2 \tag{3}$$

$$\text{for Teflon defects} \quad l = -0.0353 + 0.247 \cdot \tau_m - 0.00162 \cdot \tau_m^2$$

which approximate data in Table 2 with average accuracy 3.8 % for air and 7.5 % for Teflon.

Defect thickness could be estimated using the expressions:

$$\text{for air defects} \quad d = 0.0162 \left\{ \frac{C_m^{(2)}}{[1 - \text{Exp}(-r_d / 6)]} \right\}^{0.487} \left\{ \frac{C_m^{(2)}}{[1 - \text{Exp}(-r_d / 6)]} \right\}^{1.363} \tag{4}$$

$$\text{for Teflon defects} \quad d = 0.0422 \left\{ \frac{C_m^{(2)}}{[1 - \text{Exp}(-r_d / 6)]} \right\}^{0.768} \left\{ \frac{\tau_m}{[1 - \text{Exp}(-r_d / 4)]} \right\}^{1.630}$$

which provide average accuracy 25.7 % for air and 21.7 % for Teflon. The inversion formulas (3,4) have been used to calibrate thermal tomography data (see p.3.2).

3. "Termidge" software

3.1. General description

Principle of thermal tomography was described elsewhere [3-6]. "Termidge" software is

Table 2 Inspection parameters in the TNDT of air delaminations and Teflon inserts in the CFRP specimen

(specimen thickness 5.25 mm; specimen properties: $K_x = 1.28 [W \cdot m^{-1} \cdot K^{-1}]$;
 $K_r = 0.64 W \cdot m^{-1} \cdot K^{-1}$; $\alpha_x = 5.2 \cdot 10^{-7} [m^2 s^{-1}]$; $\alpha_r = 10.4 \cdot 10^{-7} [m^2 s^{-1}]$;
 Teflon defect thermal properties: $K = 0.25 [W \cdot m^{-1} \cdot K^{-1}]$; $\alpha = 1.1 \cdot 10^{-6} [m^2 \cdot s^{-1}]$;
 heat pulse duration $\tau_h = 5 [s]$; heat pulse power density $Q = 10^3 [W \cdot m^{-2}]$;
 heat exchange coefficient $h = 6 [W \cdot m^{-2} \cdot K^{-1}]$

Defect	r_d, mm	d, mm	l, mm	$\Delta T_m, ^\circ C$	$C_m^{(2)}$	$\tau_m(\Delta T_m), s$
Air	11.3	0.08	1.3	3.044	0.1088	6.5
			2.6	0.893	0.0319	11.8
			4.0	0.232	0.0829	16.9
		0.16	1.3	4.187	0.1496	6.7
			2.6	1.242	0.0444	12.3
			4.0	0.328	0.0117	17.4
	5.6	0.08	1.3	2.811	0.1005	6.3
			2.6	0.710	0.0254	10.7
			4.0	0.158	0.0057	15.3
		0.16	1.3	3.797	0.1357	6.4
			2.6	0.960	0.0343	11.0
			4.0	0.217	0.0078	15.6
Teflon	11.3	0.08	1.3	0.961	0.0343	6.2
			2.6	0.284	0.0102	11.5
			4.0	0.101	0.0036	20.4
		0.16	1.3	1.400	0.0500	6.2
			2.6	0.416	0.0149	11.7
			4.0	0.151	0.0054	20.7
	5.6	0.08	1.3	0.899	0.0321	6.0
			2.6	0.227	0.0081	10.4
			4.0	0.063	0.0023	16.8
		0.16	1.3	1.305	0.0466	6.1
			2.6	0.330	0.0118	10.5
			4.0	0.094	0.0034	17.0

intended to process experimental IR images taken in flash, square-pulse or periodic heating thermal test. Absolute temperature signal or normalized contrast could be used for processing. As an intermediary processing result "maxigrams" and "timegrams" are synthesized. Maxigram shows maximum temperature signal which relates to reference point selected by an operator. Hence, it provides optimum appearance of all defects independently of their depth. Timegram displays the distribution of heat transit times. They are used in the thermal tomography option. Generalized or individual calibration function could be applied in order to determine defect depth (layer coordinates in tomogram). The most accurate results appear when individual calibration functions are used, e.g. such as (2-4). The program allows to produce both "positive" and "negative" timegrams, i.e. to deal with defects which are either warmer or cooler than background. Number of processed images is limited with desired treatment time and used computer.

Defects characterization is performed using three algorithms which allow to:

- calibrate IR image in material loss (corrosion detection);
- combine both maxigram and timegram according to inversion formulas as Eqs.(2-4);
- produce thermal tomograms.

3.2. Example: tomography of defects in the CFRP specimen

Thermal tomography algorithm has been applied to IR image sequence obtained in the flash TNDT inspection of the CFRP specimen described in p.2.3 (specimen by courtesy of ONERA, France). Detailed description of this specimen and comparison of results obtained with different NDT techniques could be found in [8]. Results are shown in *figure A* (in color). The exhibited part of the specimen contained six defects located at various depths (*figure Aa*). Defects D3 and D6 partially superimposed each other in plane. Common IR image (*figure Aa*) revealed faint indications of three defects. The maxigram which must be created as an intermediary image for tomography exhibits five defects (*Fig.Ab*). Thermal tomograms have been able to separate easily all defects (*figure Ac-e*) with making clearly visible even the defect D6 at the depth 4 mm (*figure Ae*). It is worth to notice that thermal tomography is not able to show a defect which is overshadowed by another defect in plane (defects D3 and D6).

Advantage of thermal tomography relates to the fact that defects in particular layer are seen without interference with defects in other layers. Besides this, the detection of defects in thermal tomograms is more reliable due to the fact that tomography is made in time domain where signal-to-noise ratio is as a rule higher than in space domain.

Inversion Eqs.(3,4) have been applied to experimental maxigram and timegram of the CFRP specimen. Defect depth was determined with mean error 27% independently on the assumption whether the defects are air-filled or made of Teflon. Average accuracy in determining defect thickness was 24% for air defect hypothesis and 82% for Teflon hypothesis. Hence, it could be concluded that Teflon inserts in this specimen were accompanied with air delaminations.

Acknowledgments

Authors would like to thank Dr. D. Balageas of ONERA (France) for fruitful discussion on the inspection results related to the standard CFRP specimen.

REFERENCES

- [1] VAVILOV (V.) and TAYLOR (R.). - *Theoretical and practical aspects of the thermal NDT of bonded structures*. In: Res.Techn.in NDT, ed. by R.Sharpe, Academic Press, London, U.K., 1982, vol. 5, pp.239-280.
- [2] VAVILOV (V.). - *Thermal non destructive testing: short history and state-of-art*. Proc. of the Eurotherm Seminar 27 "Quantitative Infrared Thermography-QIRT 92", July 7-9, 1992, Chatenay-Malabry, France, pp.179-194.
- [3] VAVILOV (V.), AHMED (T.), JIN (J.), THOMAS (R.L.) and FAVRO (L.D.). - *Dynamic thermal tomography: new NDE technique to reconstruct inner solids structure using multiple IR image processing*. Rev. of Progress in Quant. NDE, ed. by D.Thompson and D.Chimenti, vol. 11A, 1992, Plenum Press, N.Y., U.S.A., pp.4525-4532.
- [4] VAVILOV (V.), DEGIOVANNI (A.), DIDIERJEAN (S.), HOULBERT (A.S.) and MAILLET (D.). - *Thermal NDT and tomography of carbon epoxy plastics*. Sov.J.NDT, 1991, No.9, pp.3-14.
- [5] VAVILOV (V.), BISON (P.), BRESSAN (C.), GRINZATO (E.) and MARINETTI (S.). - *Some new ideas in dynamic thermal tomography*. See[2], pp. 259-265.
- [6] VAVILOV (V.), MALDAGUE (X.), DUFORT (B.), ROBITAILLE (F.) and PICARD (J.). - *Thermal NDT of carbon epoxy composites: detailed analysis and data processing*. NDT&E Intern., 1993, vol.26, No.2, pp.85-95.
- [7] GRINZATO (E.), BISON (P.), MARINETTI (S.) and VAVILOV (V.). - *Nondestructive evaluation of delaminations in frescos plaster using transient infrared thermography*. Res. Nondestr. Eval., 1994, vol. 5, n° 4, pp. 257-271.
- [8] KRAPEZ (J.C.), BALAGEAS (D.), DEOM (A.) and LEPOUTRE (F.). - *Early Detection by Stimulated Infrared Thermography. Comparison with Ultrasonics and Holo/Shearography*. In: "Advances in Signal Processing for NDE of Materials", ed. by X. Maldague, NATO ASI Series, Series E: Applied Sciences, Kluwer Academic Publishers, Vol.262, pp.303-321.